Langmuir

Article

pubs.acs.org/Langmuir

Concentration Dependence of the Interfacial Tension for Aqueous Two-Phase Polymer Solutions of Dextran and Polyethylene Glycol

Yonggang Liu,*,† Reinhard Lipowsky, and Rumiana Dimova*

Department of Theory and Bio-Systems, Max Planck Institute of Colloids and Interfaces, Science Park Golm, 14424 Potsdam, Germany

ABSTRACT: We studied the interfacial tension between coexisting phases of aqueous solutions of dextran and polyethylene glycol. First, we characterized the phase diagram of the system and located the binodal. Second, the tie lines between the coexisting phases were determined using a method that only requires measuring the density of the coexisting phases. The interfacial tension was then measured by a spinning drop tensiometer over a broad range of polymer concentrations close to and above the critical point. In this range, the interfacial tension increases by 4 orders of magnitude with increasing polymer concentration. The scaling exponents of the interfacial tension, the correlation length, and order parameters were evaluated and showed a crossover behavior depending on the distance to the critical concentration. The scaling exponent of the interfacial tension attains the value 1.50 ± 0.01 further away from the critical point, in good agreement with mean field theory, but the increased value 1.67 ± 0.10 closer to this point, which disagrees with the Ising value 1.26. We discuss possible reasons for this discrepancy. The composition and density differences between the two coexisting phases, which may be taken as two possible order parameters, showed the expected crossover from mean field behavior to Ising model behavior as the critical point is approached. The crossover behavior of aqueous two-phase polymer solutions with increasing concentration is similar to that of polymer solutions undergoing phase separation induced by lowering the temperature.

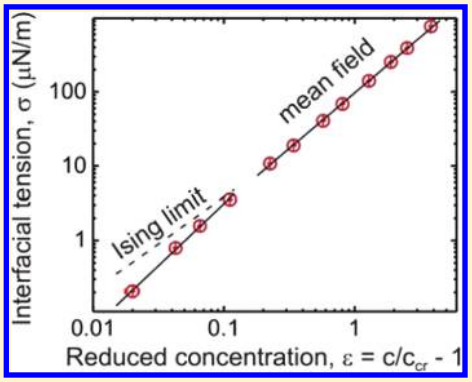

INTRODUCTION

Phase separation can occur when solutions of two different polymers are mixed above a certain concentration. Here, we study the demixing of aqueous solutions of dextran and polyethylene glycol (PEG). Two immiscible phases are obtained, with one phase rich in dextran and the other one rich in PEG. Because of their simplicity and biocompatibility, such aqueous two-phase systems (ATPSs) are widely used in separation of biomolecules, viruses, and cells.[1] When biological materials are mixed in ATPSs, they can selectively adsorb at the liquid−liquid interface. The PEG−dextran polymer systems provide a particularly mild environment for biomolecules and cells because the interfacial tensions found in these systems are extremely low (about 1−100 μN/m).[2] In such polymeric two-phase systems, no detectable denaturation of proteins occurs, in contrast to two-phase systems based on solutions of small molecules and characterized by higher interfacial tensions, typically on the order of tens of millinewtons per meter.

A large number of studies on the properties of the PEG−dextran system have been reported in the past couple decades; see, e.g., refs 3−6. However, because of the potential biotechnological application of this aqueous polymer system for protein isolation and drug delivery, there is a renewed interest toward quantitative characterization of the system phase behavior. ATPSs containing PEG and dextran are also employed as basic models for the cytoplasm exhibiting macromolecular crowding.[7] Furthermore, as we will discuss below, a number of interesting phenomena have been observed on model membranes in contact with PEG−dextran ATPSs, the detailed interpretation of which requires precise data about the concentration dependence of the interfacial tension.

Recently, Keating et al.[8] demonstrated the possibility of enclosing ATPSs in giant unilamellar vesicles.[9] In their studies, phase separation was induced by lowering the temperature.[8] An alternative method is provided by increasing the polymer concentration within the vesicle by deflation.[10] Dynamic microcompartmentation of biomolecules between the enclosed phases was found to resemble similar partitioning behavior as proposed in the cytoplasm of living cells.[11] Interesting phenomena associated with the phase separation process, such as wetting transitions,[10] vesicle budding,[12,13] fission of vesicles,[14] and formation of membrane nanotubes,[15] were reported. In all of these cases, the observed processes were governed by the interplay between the interfacial tension of the polymer phases and the membrane tension. Thus, acquiring precise and reproducible data on the interfacial tension over a wide range of polymer concentrations is of fundamental importance to understand the phase separation of ATPSs within vesicles and its role in membrane transformations.

In the present paper, we report results from measurements of the interfacial tension of aqueous two-phase polymer solutions of dextran and PEG over a wide range of polymer

Received: December 2, 2011
Revised: January 30, 2012
Published: January 31, 2012

concentrations above the critical concentration of phase separation. The explored concentrations cover those of biomacromolecules in cells. The scaling relation of the interfacial tension, order parameters, including the density difference and the concentration difference, and the correlation length with the distance to the critical concentration was established and compared with the predictions from mean field theory and the critical behavior in the three-dimensional Ising model. The deduced scaling exponents obtained in this work refer to the effective critical exponents, which become the true critical exponents in the asymptotic regime very close to the critical point. We also report the exact phase diagram, including the tie lines, and propose a relatively simple method for locating the tie lines in the phase diagram based on density measurements.

MATERIALS AND METHODS

Dextran from the bacterium *Leuconostoc mesenteroides* (molar mass between 400 and 500 kg/mol) and PEG (molar mass 8 kg/mol) were purchased from Sigma-Aldrich. The polydispersity was 1.83 for dextran and 1.11 for PEG as measured by gel permeation chromatography.[10] Their radii of gyration, R_g, were 21 and 4.05 nm, respectively.[16,17]

Concentrated stock solutions of dextran and PEG (10−20% by weight) were prepared by dissolving polymers in deionized water. The binodal of dextran and PEG aqueous solution was determined by cloud-point titration at 24 ± 0.5 °C both from the one-phase region to the two-phase region and vise versa.[1] Titration was also employed to locate the critical point at which the phase volumes are equal as one approaches the binodal in the two-phase region.[18] A certain concentration of dextran solution was prepared by adding water to the dextran stock solution in a 10 mL flask. Then PEG stock solution was added dropwise into the flask followed by shaking. The titration continued until the solution became turbid. The mass of each stock solution and water was measured by a balance. Alternatively, mixtures of dextran and PEG solutions with different polymer weight ratios were prepared in the two-phase region in 10 mL measuring cylinders. Afterward, water was added stepwise until the solution in the cylinders became clear. At each step, the system was allowed to equilibrate for a couple of hours or days until complete phase separation, and the volumes of the coexisting phases were measured.

To construct the tie lines, mixtures of dextran and PEG solutions were prepared in the two-phase region in 50 mL separating funnels by keeping the weight ratio between dextran and PEG equal to that at the critical point. The solutions were shaken by hand to ensure good mixing of the polymers. The samples were kept at a temperature of 24 ± 0.5 °C for several days before the PEG-rich phase was taken from the upper outlet and the dextran-rich phase was taken from the lower one. The density of each separated phase was measured at 24 ± 0.001 °C with a density meter (DMA5000, Anton Paar) with a resolution of 5 μg/mL. The refractive index was measured at the same temperature with an RE50 refractometer (Mettler Toledo) with an accuracy of 0.00005 at 589 nm.

The interfacial tension between the coexisting dextran-rich and PEG-rich phases corresponding to a certain tie line was measured using a SITE100 spinning drop tensiometer (Krüss). A 1−2 μL droplet of the solution of the PEG-rich phase was injected into a transparent glass capillary (with a diameter of 3.5 mm) filled with the denser solution of the dextran-rich phase. The horizontally aligned capillary rotated at a certain speed ω between 500 and 15 000 rpm, and the lighter droplet became elongated along the axis of rotation. The interfacial tension, σ, between the two phases was calculated from the Vonnegut equation at sufficiently high rotation speed when the length of the droplet exceeded 4 times its equatorial diameter.[19,20] This equation has the form

$$\sigma = \frac{\Delta\rho\omega^2 r^3}{4} \quad (1)$$

where $\Delta\rho$ is the density difference between the coexisting phases and r is the equatorial radius of the ellipsoidal droplet shape. This radius was calibrated by measuring the diameter of a stiff cylindrical stick in the capillary filled with the same solution of the dextran-rich phase.

RESULTS AND DISCUSSION

Phase Diagram and Critical Point. The binodal of the aqueous solution of dextran and PEG is shown in Figure 1. The solution undergoes phase separation at a total polymer weight fraction above several weight percent. Titrations starting from either the one-phase or the two-phase region yielded identical phase boundaries. A series of polymer solutions in the two-phase region at certain weight ratios w_d/w_p between dextran and PEG were prepared, and the volume fraction of each phase was measured when approaching the binodal by adding water gradually. In the following, we will refer to such a series of polymer solutions as a titration trajectory (see Figure 1) characterized by a fixed value of w_d/w_p. Figure 2 shows the

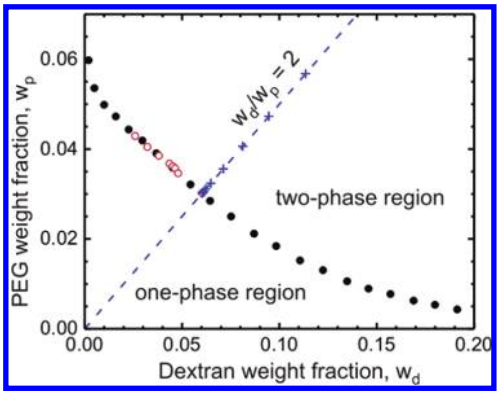

Figure 1. Binodal of the aqueous solution of dextran and PEG at 24 ± 0.5 °C obtained by titration from the one-phase to the two-phase region (solid circles) and vice versa (open circles). The "+" symbols are experimental points along the titration trajectory with $w_d/w_p = 2.0$ (dashed line). The intersection of such a trajectory with the binodal defines the polymer weight fraction w_{bi}.

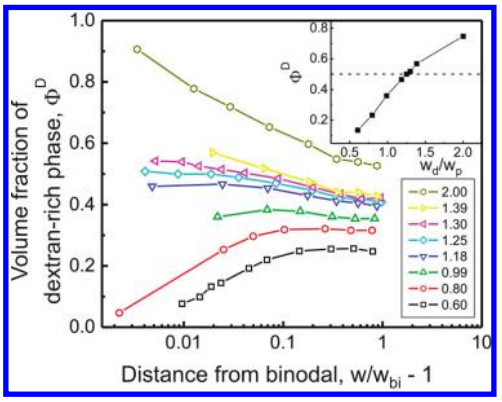

Figure 2. Volume fraction Φ^D of the dextran-rich phase as a function of the normalized distance from the binodal, $w/w_{bi} - 1$, for polymer solutions of different weight ratios w_d/w_p between dextran and PEG ranging from 0.60 to 2.00. See the lower inset with the color code. The upper inset shows the dependence of the volume fraction Φ^D on the weight ratio w_d/w_p very close to the phase boundary at $w/w_{bi} = 1.02$. For $\Phi^D = 0.50$ (dashed line), the polymer weight ratio $w_d/w_p = 1.25$ was found.

dx.doi.org/10.1021/la204757z | Langmuir 2012, 28, 3831−3839

volume fraction Φ^D of the dextran-rich phase as a function of the normalized distance from the binodal $w/w_{bi} - 1$. Here w is the total polymer weight fraction, $w = w_d + w_p$, and w_{bi} is the polymer weight fraction defined by the intersection of a certain titration trajectory (i.e., a certain weight ratio w_d/w_p) with the binodal. The evolution of the volume fraction Φ^D was measured at different weight ratios w_d/w_p ranging from 0.60 to 2.00. When approaching the binodal along the titration trajectory, the two phases were found to have equal volumes ($\Phi^D = 0.50$) for weight ratio $w_d/w_p = 1.25$; see the inset in Figure 2. Carefully studying the phase behavior of solutions close to the binodal by keeping the weight ratio $w_d/w_p = 1.25$ gave the composition of the critical point with a total polymer weight fraction of $w_{cr} = 0.0812 \pm 0.0002$.

We then examined the density properties of the polymer solutions with fixed weight ratio $w_d/w_p = 1.25$ and with total polymer weight fraction in the range $w_{cr} < w < 0.36$. The coexisting dextran-rich and PEG-rich phases were separated, and their densities were measured. The results are shown in Figure 3. The densities of pure dextran solutions and pure PEG

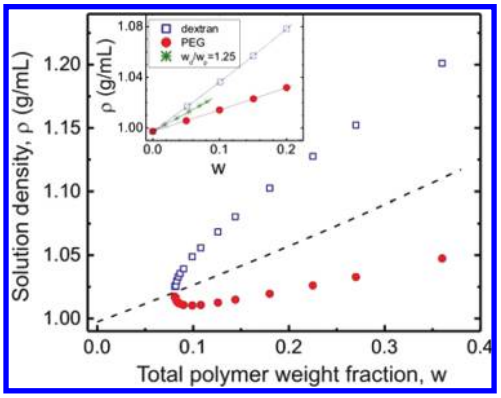

Figure 3. Densities of the coexisting dextran-rich (open squares) and PEG-rich (solid circles) phases for polymer solutions with weight ratio $w_d/w_p = 1.25$ as functions of the total initial polymer weight fraction w. The dashed line is the calculated density of the polymer solution with $w_d/w_p = 1.25$. In the inset, the densities of pure dextran and pure PEG solutions and their mixtures with $w_d/w_p = 1.25$ in the one-phase region are plotted as functions of the total polymer weight fraction w. The lines are fits to eq 2 with specific volumes $v_d = 0.62586 \pm 0.00046$ mL/g and $v_p = 0.83494 \pm 0.00043$ mL/g.

solutions and their mixtures with weight ratio $w_d/w_p = 1.25$ in the one-phase region are also shown in the inset of Figure 3. Assuming that the specific volume of the polymer solution is the sum of the contributions from each component, one can relate the total mass density ρ of the polymer solution to the weight fraction of each component by

$$1/\rho = (1 - w_d - w_p)v_s + w_d v_d + w_p v_p \quad (2)$$

where the specific volume of water $v_s = 1.00271$ mL/g at 24 °C and v_d and v_p are the specific volumes of dextran and PEG, respectively. Equation 2 was found to fit the data very well in the region of polymer weight fractions up to $w = 0.20$. The best fits were obtained for the specific volumes $v_d = 0.62586 \pm 0.00046$ mL/g and $v_p = 0.83494 \pm 0.00043$ mL/g. These values are in very good agreement with values reported in ref 21.

Locating the Tie Lines in the Phase Diagram. We proceeded with characterizing the compositions of the phases in the phase-separated system as described by the tie lines in the phase diagram. A variety of methods for tie line determination have been explored in the literature based on the use of different experimental techniques; see, e.g., ref 22. Here, we propose a relatively simple approach based on density measurements of the phases.

From the measured mass densities of the coexisting dextran-rich (D) and PEG-rich (P) phases, ρ^D and ρ^P, respectively, one can deduce the composition of each phase. After rewriting eq 2 for each of the phases, for the PEG weight fractions in the dextran-rich and PEG-rich phases, w_p^D and w_p^P, respectively, we obtain the following dependencies:

$$w_p^D = \frac{1}{v_p - v_s}\left[\frac{1}{\rho^D} - v_s - (v_d - v_s)w_d^D\right] \quad (3a)$$

$$w_p^P = \frac{1}{v_p - v_s}\left[\frac{1}{\rho^P} - v_s - (v_d - v_s)w_d^P\right] \quad (3b)$$

where w_d^D and w_d^P are the dextran weight fractions in the dextran-rich and PEG-rich phases, respectively. For fixed densities ρ^D and ρ^P, eqs 3a and 3b represent isopycnic (constant density) lines in the (w_d, w_p) plane. The intersections of these lines with the binodal provide the compositions of the coexisting phases, i.e., the end points of the tie line. To apply this rule, the binodal curve was either interpolated by polynomial fitting or extrapolated linearly on a logarithmic scale.

In Figure 4, we illustrate the approach of locating the tie lines in the phase diagram in the following way. As an example, we

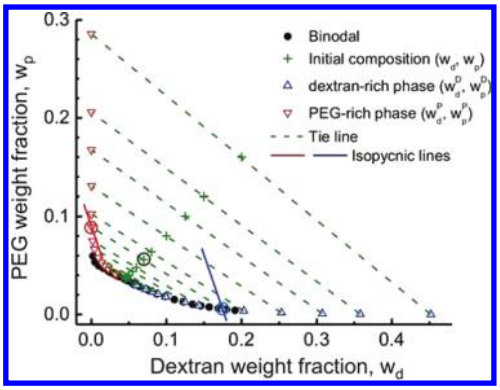

Figure 4. Tie lines in the dextran−PEG phase diagram. The solid circles show the data for the experimentally measured binodal (same data as in Figure 1). The compositions of the initial solutions (with weight ratio $w_d/w_p = 1.25$) for which the phase densities after phase separation were measured are indicated by "+" symbols. The end points of the respective tie lines consist of upward-pointing triangles indicating the compositions of the dextran-rich phases and downward-pointing triangles indicating the compositions of the PEG-rich phases. The solid lines represent two examples of isopycnic lines calculated following eqs 3a and 3b for the initial solution composition indicated with an encircled "+" symbol in the graph: $(w_d, w_p) = (0.0700, 0.0560)$. The intersections of the isopycnic lines with the binodal yield the compositions of the two phases, also encircled.

consider the polymer solution with initial composition $(w_d, w_p) = (0.0700, 0.0560)$; see the encircled "+" symbol in Figure 4. For this system, the measured densities had the values $\rho^D = 1.068378$ g/mL for the dextran-rich phase and $\rho^P = 1.012587$ g/mL for the PEG-rich phase. The isopycnic lines for this polymer solution calculated with eqs 3a and 3b are also plotted in Figure 4. Their intersections with the extrapolated or

dx.doi.org/10.1021/la204757z | Langmuir 2012, 28, 3831−3839

interpolated binodal line lead to the compositions $(w_d^D, w_p^D) = (0.1746, 0.0057)$ and $(w_d^P, w_p^P) = (0.0006, 0.0890)$ of the dextran-rich and PEG-rich phases, respectively. Note that every isopycnic line has, in general, two intersection points with the binodal. The decision about the correct one is made on the basis of the initial solution composition and the reasoning that the dexran-rich phase has the higher dextran concentration. The tie lines found using this approach agree very well with previously reported data for the dextran−PEG system (with similar molar masses of the polymers) measured at temperatures between 20 and 25 °C.[2,23,24]

The precision of this construction method for the tie lines depends on the accuracy of locating the binodal. As described above, for plotting a tie line, we generally used the two intersection points of the isopycnic lines with the binodal. The fact that the coordinates (w_d, w_p) of the initial compositions of the measured polymer solutions (indicated by "+" symbols in Figure 4) lie very close to the corresponding tie lines (the distances to the tie lines are less than 0.0006) demonstrates the relatively high accuracy of our procedure.

For solution compositions close to the critical point, where the isopycnic lines of the PEG-rich phases are almost tangential to the binodal, the compositions (w_d^P, w_p^P) cannot be determined in a reliable manner from the density ρ^P of the PEG-rich phase alone. In these cases, we first located the composition of the dextran-rich phase. Then the composition of the PEG-rich phase was estimated from the intersection of the isopycnic line of the PEG-rich phase with a line passing through the coordinates of the initial solution composition (w_d, w_p) and those of the dextran-rich phase composition (w_d^D, w_p^D). This procedure implied a small mismatch (less than 0.005) between the experimentally measured binodal and the PEG-rich phase end points of the tie lines.

To check the validity of the compositions of the tie line end points as determined by the procedure just described, the refractive indices of the coexisting phases were measured. The results are shown in Figure 5. The obtained data were compared with values calculated from the compositions as determined on the basis of the measured phase density as described above. The refractive indices of the dextran-rich or PEG-rich phase, n^D or n^P, respectively, are related to the polymer concentration in these phases via[1]

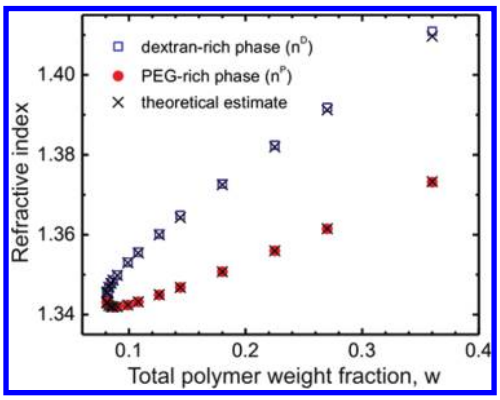

Figure 5. Refractive indices of the coexisting dextran-rich phase, n^D (open squares), and PEG-rich phase, n^P (solid circles), for polymer solutions with weight ratio $w_d/w_p = 1.25$ as functions of the total initial polymer weight fraction w. The theoretical estimates ("×" symbols) were calculated from the phase compositions determined in Figure 4 following eqs 4a and 4b as explained in the text.

$$n^D = n_s + [(dn/dc)_d w_d^D + (dn/dc)_p w_p^D]\rho^D \quad (4a)$$

$$n^P = n_s + [(dn/dc)_d w_d^P + (dn/dc)_p w_p^P]\rho^P \quad (4b)$$

where the water or solvent refractive index is $n_s = 1.3326$. The values of the refractive index increments $(dn/dc)_d$ and $(dn/dc)_p$ were measured independently for pure dextran and PEG solutions at several weight fractions up to 0.20. These increments were found to be $(dn/dc)_d = 0.142$ mL/g for dextran and $(dn/dc)_p = 0.136$ mL/g for PEG in aqueous solution. These values are in very good agreement with values reported in ref 25.

The refractive indices of the coexisting phases calculated according to eqs 4a and 4b and using the phase compositions (w_d^D, w_p^D) and (w_d^P, w_p^P) estimated in Figure 4 are also plotted in Figure 5 ("×" symbols). The theoretically estimated values are very close to the experimentally measured data, demonstrating that the tie lines in Figure 4 have been accurately determined. Small deviations are detected for a few points of the dextran-rich phase at high polymer concentrations where nonlinear effects should be present.

PEG−water and dextran−water mixtures exhibit a lower and upper critical solution temperature, respectively. Thus, the phase behavior of the PEG−dextran system in water is temperature dependent. Binodals measured at three different temperatures for a system similar to the one studied here were reported in ref 8. The temperature dependence of the phase diagram was employed to induce phase separation within giant unilamellar vesicles loaded with the polymer mixture in the single phase.[8,11] In principle, the tie line construction method as described above can be used to study the temperature dependence of the phase boundaries. In practice, such an extended study of the phase diagram is rather time-consuming and has not been pursued here.

Apart from determining the tie lines of the solutions, the data obtained for the phase densities and refractive indices can also be used to locate the critical concentration. This is demonstrated in Figure 6, which shows the density difference and the refractive index difference of the coexisting phases, $\Delta\rho = \rho^D - \rho^P$ and $\Delta n = n^D - n^P$, respectively, as functions of the total initial polymer weight fraction. Both $\Delta\rho$ and Δn converge to zero at the critical weight fraction $w_{cr} = 0.0812 \pm 0.0002$. This value is in excellent agreement with the one that we obtained from the measured volume fractions of the phases; see the previous section.

Interfacial Tension. The interfacial tension σ between the coexisting dextran-rich and PEG-rich phases was measured by a spinning drop tensiometer. Figure 7 illustrates the principle of the measurement with one example for initial polymer weight fraction $(w_d, w_p) = (0.0700, 0.0560)$. An apparent interfacial tension, σ_{app}, was calculated from the shape of the drop using eq 1. The rotation angular frequency ω was varied between 500 and 14 000 rpm. The PEG-rich phase droplet is initially spherical and at low angular frequency is only slightly deformed by the small centrifugation force. As the angular frequency increases, the droplet becomes increasingly elongated along the rotation axis, as characterized by the long axis, l, and the equatorial radius, d, of the droplet decreases. At aspect ratios $l/d > 4$, the apparent interfacial tension is constant and provides an estimate for the true interfacial tension σ. In principle, the dependence of the apparent interfacial tension in the range of smaller droplet lengths can also be used to extract the true interfacial tension following an approach given in ref 20. Here

dx.doi.org/10.1021/la204757z | Langmuir 2012, 28, 3831−3839

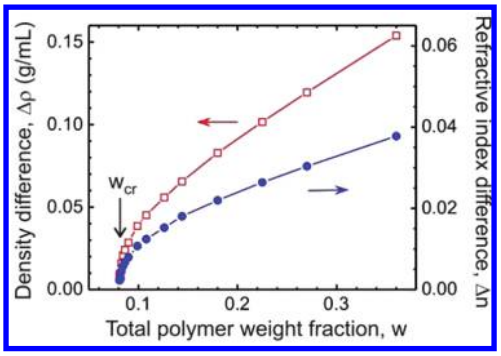

Figure 6. Density difference, $\Delta\rho = \rho^D - \rho^P$ (open squares), and refractive index difference, $\Delta n = n^D - n^P$ (solid circles), for polymer solutions with weight ratio $w_d/w_p = 1.25$ as functions of the total initial polymer weight fraction w. Both $\Delta\rho$ and Δn vanish at the critical concentration $w_{cr} = 0.0812 \pm 0.0002$.

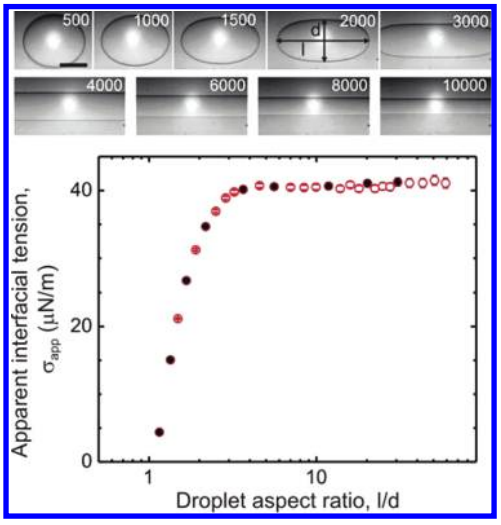

Figure 7. Apparent interfacial tension σ_{app} between the coexisting phases with an initial polymer weight fraction of $(w_d, w_p) = (0.0700, 0.0560)$ as a function of the aspect ratio l/d as measured for the PEG-rich phase droplet at varied rotation speed. The long axis of the droplet is parallel to the rotation axis. The measurement error is smaller than the symbol size as shown by the error bars. The apparent interfacial tension, which is calculated following eq 1, yields the intrinsic interfacial tension σ at high angular frequency. The images above the graph show the PEG-rich phase droplet at rotation speeds of 500, 1000, 1500, 2000, 3000, 4000, 6000, 8000, and 10000 rpm (corresponding to the solid circles in the graph). The length and diameter of the droplet are indicated on the image at 2000 rpm. The scale bar is 0.5 mm.

we used eq 1 for this purpose. Measurements on several different droplets gave the interfacial tension $\sigma = 40.8 \pm 0.5$ μN/m.

The polymer weight fraction closest to the critical point that we could explore was $w = 0.0828$, and the corresponding interfacial tension was found to be $\sigma = 0.21$ μN/m. Increasing the polymer weight fraction to $w = 0.360$ raised the interfacial tension by 4 orders of magnitude to 769 μN/m. At polymer weight fractions lower than 0.0828, i.e., closer to the critical point, the measurement is rather difficult and no accurate data were obtained. In Figure 8A, we present the collected results for the interfacial tension as a function of the total polymer concentration c. Note that we chose to present the data in terms of the total polymer mass density or concentration $c \equiv$

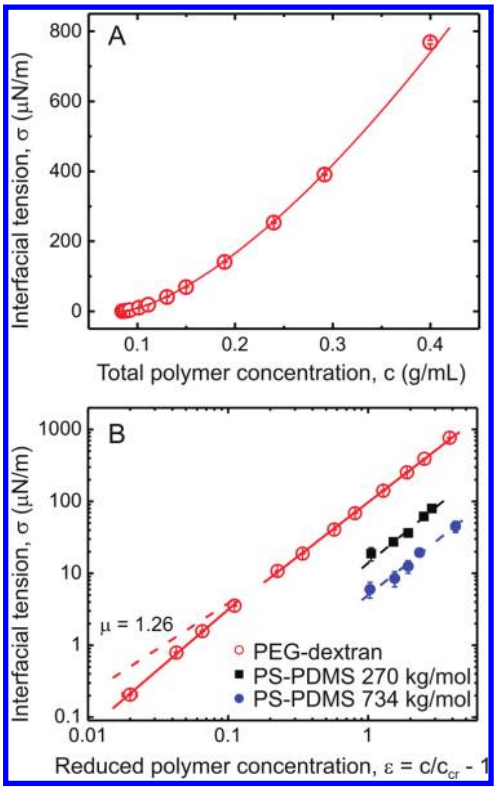

Figure 8. Interfacial tension between the coexisting dextran-rich and PEG-rich phases as functions of (A) the total initial polymer concentration and (B) the reduced polymer concentration $\varepsilon = c/c_{cr} - 1$. The solid lines are fits to $\sigma = \sigma_0\varepsilon^\mu$ with $\sigma_0 = 146.3 \pm 2.8$ μN/m and $\mu = 1.67 \pm 0.10$ for $0.02 < \varepsilon < 0.12$, as well as $\sigma_0 = 97.2 \pm 0.7$ μN/m and $\mu = 1.50 \pm 0.01$ for $0.2 < \varepsilon < 3$. The red dashed line shows the expected asymptotic behavior with $\mu = 1.26$. In (B), the solid squares and circles show two additional sets of data reported in ref 35 for the two-phase system polystyrene−poly(dimethylsiloxane) (PS−PDMS) dissolved in toluene with polymer molar masses of 270 and 734 kg/mol, respectively. The black and blue dashed lines are fits to the data with $\mu = 1.60 \pm 0.18$ and 1.54 ± 0.13, respectively.

$w\rho$ in units of grams per milliliter instead of the dimensionless weight fraction w, because available theoretical models use this presentation. The critical concentration is then given by $c_{cr} = w_{cr}\rho_{cr} = 0.0829 \pm 0.0002$ g/mL.

Scaling Exponents for the Order Parameters, Interfacial Tension, and Correlation Length. Scaling exponents associated with the singular behavior of various thermodynamic properties, such as the susceptibility χ and the correlation length ξ, and the vanishing of the order parameters and the interfacial tension σ, at temperature T close to the critical temperature T_c, have been determined for various polymer solutions.[26,27] The observed singular behavior could be described by the three-dimensional Ising model, by the mean field theory, or as crossover behavior, depending on the explored region of the reduced temperature $\tau = |1 - T/T_c|$. For example, the divergence of the susceptibility $\chi \sim \tau^{-\gamma}$ and the correlation length $\xi \sim \tau^{-\nu}$ showed a crossover behavior from the Ising model to the mean field with the scaling exponents γ and ν changing from 1.24 to 1 and from 0.63 to 1/2,[28,29] respectively. The crossover was located at the reduced temperature τ, at which the correlation length is on the order of the radius of gyration of the polymer. The vanishing of the concentration difference of the coexisting phases $\Delta\phi \sim \tau^\beta$ showed a crossover from Ising model behavior with $\beta = 0.326$

dx.doi.org/10.1021/la204757z | Langmuir 2012, 28, 3831−3839

to mean field behavior characterized by $\beta = 1/2$.[30] However, crossover of the scaling exponent μ describing the vanishing of the interfacial tension of the coexisting phases $\sigma \sim \tau^{\mu}$ has not been observed, although values both close to the Ising model prediction of $\mu = 1.26$ (experimentally observed values lie in the region 1.17−1.35) and close to the mean field theory prediction of $\mu = 3/2$ (experimentally observed values lie in the region 1.30−1.60) have been reported.[27,31,32]

Here we apply a similar approach to determine the scaling exponents of the order parameters, the interfacial tension, and the correlation length with the distance to the critical point, which in our case is the reduced concentration:

$$\varepsilon \equiv c/c_{cr} - 1 \tag{5}$$

In Figure 9, the order parameters of the coexisting phases, namely, the composition difference Δc, which is defined by the

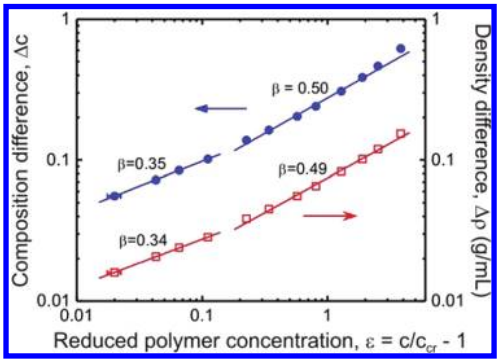

Figure 9. Composition difference Δc (solid circles) and density difference $\Delta\rho$ (open squares) of the coexisting phases as functions of the reduced polymer concentration ε. In the concentration range $0.02 < \varepsilon < 0.12$, the fits to the data give for the scaling exponent β a value of 0.337 ± 0.018 as estimated from the density difference dependence or 0.351 ± 0.018 as estimated from the composition difference dependence, while in the range $0.2 < \varepsilon < 3$ we obtain 0.491 ± 0.014 from the density difference dependence or 0.503 ± 0.018 from the composition difference dependence.

length of the tie line expressed in terms of the PEG and dextran concentrations $c_p \equiv w_p\rho$ and $c_d \equiv w_d\rho$, and the density difference $\Delta\rho$ are plotted as functions of the reduced concentration $\varepsilon = c/c_{cr} - 1$ with the critical concentration c_{cr} = 0.0829 ± 0.0002 g/mL as measured in this study. The scaling exponent β in $\Delta\rho \sim \varepsilon^{\beta}$ or $\Delta c \sim \varepsilon^{\beta}$ shows two different values: (i) in the concentration range $0.02 < \varepsilon < 0.12$ (regime I), we obtain 0.337 ± 0.018 as estimated from the density difference dependence or 0.351 ± 0.018 as estimated from the composition difference dependence, and (ii) in the range $0.2 < \varepsilon < 3$ (regime II), we obtain 0.491 ± 0.014 from the density difference dependence or 0.503 ± 0.018 from the composition difference dependence; see Figure 9. These values are in good agreement with the Ising value $\beta = 0.326$ for regime I and the mean field value $\beta = 1/2$ for regime II. Such a crossover is analogous to previous results obtained with polymer solution when approaching the critical point by lowering the temperature.[30]

In Figure 8B, we fit the dependence of the interfacial tension on the reduced concentration to the power law dependence $\sigma = \sigma_0\varepsilon^{\mu}$. The data show two regimes as well: (regime I) σ_0 = (146.3 ± 2.8) μN/m and $\mu = 1.67 \pm 0.10$ for $0.02 < \varepsilon < 0.12$ and (regime II) σ_0 = (97.2 ± 0.7) μN/m and $\mu = 1.50 \pm 0.01$ for $0.2 < \varepsilon < 3$. The large error bar of μ in regime I mainly arises from the error in the critical concentration. Furthermore, only four data points covering about 1 order of magnitude were used for fitting. The scaling exponent $\mu = 1.50 \pm 0.01$ characterizing regime II corresponds exactly to the predictions of the mean field theory, indicating that at reduced concentration $\varepsilon > 0.2$ the compositional fluctuations are screened out by the radius of gyration of the polymer. This observation is further supported by the following discussion of the correlation length. The values obtained for the scaling exponents of the order parameters (see Figure 9) suggest that regime I corresponds to the critical region where mean field theory fails and Ising model behavior is expected.[33] However, in regime I we observe $\mu = 1.67 \pm 0.10$ for the scaling exponent of the interfacial tension, which is higher than the Ising value $\mu = 1.26$. We will discuss this discrepancy further below.

The concentration dependence of the interfacial tension of demixed polymer blends in solution has been theoretically studied before.[34,35] Mean field theory predicted an exponent of $\mu = 3/2$,[34] while scaling considerations gave a slightly different value of 1.65.[35] In Figure 8B, two sets of interfacial tension data for the two-phase system polystyrene−poly(dimethylsiloxane) dissolved in toluene (in each data set both polymers had the same molar mass) reported in ref 35 are also shown. Fitting of the data to $\sigma = \sigma_0(c/c_{cr} - 1)^{\mu}$ yields $\mu = 1.60 \pm 0.18$ and 1.54 ± 0.13 for two polymer pairs of different molar masses. These values are in reasonable agreement with the mean field theory prediction since the reduced concentration $\varepsilon > 1$ for these experiments. Other experiments on the interfacial tension of a demixed aqueous solution of dextran and gelatin showed a similar value of 1.5 ± 0.1 for the scaling exponent μ.[36]

The correlation length ξ of the composition fluctuations was extracted from the interfacial tension by two methods. The first method is based on the Ornstein−Zernike relation:[34]

$$\xi = \frac{\rho_0 b^2 k_B T(\phi - \phi_{cr})}{3\sigma} \tag{6}$$

where the monomer number density $\rho_0 = N_A\rho/M_u$, with N_A the Avogadro number, ρ the density of pure polymer (dextran or PEG), and M_u the molar mass of the Kuhn monomer (M_u = 162 g/mol for dextran and M_u = 88 g/mol for PEG), the Kuhn length b = 0.44 nm for dextran[37] and 0.76 nm for PEG,[38] k_B is the Boltzmann constant, and T is the temperature. The total polymer volume fraction $\phi = (5/9\nu_d + 4/9\nu_p)c = 0.7188c$ and the total polymer volume fraction at the critical point $\phi_{cr} = 0.7188c_{cr}$, so that $\phi - \phi_{cr} \sim \varepsilon$. For the values of the monomer density ρ_0 and the Kuhn length b we used the geometrical means of the values of dextran and PEG. The second method to extract the critical behavior of the correlation length ξ is based on the scaling relation

$$\xi \sim \sqrt{\frac{k_B T}{\sigma}} \equiv \xi_{\sigma} \tag{7}$$

between this length scale and the interfacial tension σ, a relation that should be valid sufficiently close to the critical point.[39]

It should be noted that the first method is derived from the classical mean field theory, while the second approach follows the scaling theory of critical phenomena. Both methods lead to power laws of the form $\xi \sim \varepsilon^{-\nu}$ for the correlation length ξ as a function of the reduced concentration ε but with different scaling exponents ν. The comparison of the scaling exponent ν with the theoretical values provides a way to test the correspondence between the experimental data and the

dx.doi.org/10.1021/la204757z | Langmuir 2012, 28, 3831−3839

different theories. Figure 10 shows the correlation length of the composition fluctuation ξ calculated from the measured

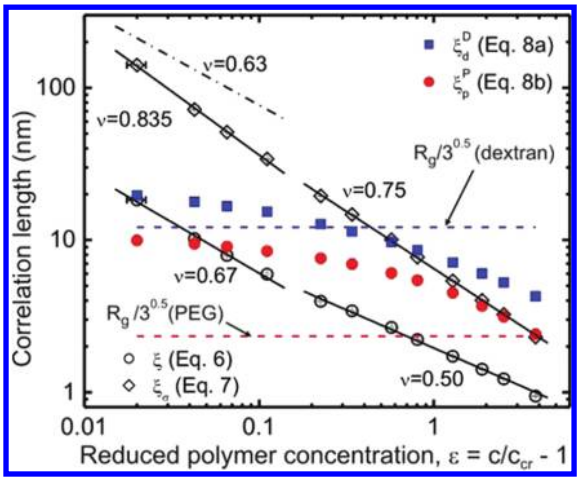

Figure 10. Correlation lengths as a function of the reduced polymer concentration ε. The correlation length ξ was calculated via eq 6 (open circles) and by ξ_σ in eq 7 (open tilted squares). The correlation lengths ξ_d^D of the concentration fluctuations of dextran in the dextran-rich phase (solid squares) and ξ_p^P of PEG in the PEG-rich phase (solid circles) were estimated following eqs 9a and 9b. The horizontal dashed lines indicate the normalized radii of gyration of dextran ($R_g/3^{1/2} \cong$ 12.1 nm) and of PEG ($R_g/3^{1/2} \cong$ 2.34 nm) in dilute aqueous solutions. The dashed−dotted line shows the expected asymptotic behavior with $\nu = 0.63$.

interfacial tension σ according to eqs 6 and 7. The correlation length calculated from eq 7 is several times larger than that following the mean field estimates from eq 6. Two regimes are observed for the mean field estimates as obtained from eq 6: (i) closer to the critical concentration, in the range $0.02 < \varepsilon < 0.12$, the scaling exponent $\nu = 0.670 \pm 0.041$, and (ii) further away, in the range $0.2 < \varepsilon < 3$, the scaling exponent $\nu = 0.500 \pm 0.009$. The latter value agrees with the value $\nu = 1/2$ as predicted from the mean field theory, indicating that mean field behavior shows up in the region far away from the critical point at $\varepsilon > 0.2$. Closer to the critical point at $\varepsilon < 0.12$, compositional fluctuations become important and the mean field theory fails, leading to an increase of the exponent ν. Such a crossover was also observed for the exponents of the correlation length calculated from eq 7: (i) closer to the critical concentration, in the range $0.02 < \varepsilon < 0.12$, $\nu = 0.835 \pm 0.051$, and (ii) further away, in the range $0.2 < \varepsilon < 3$, $\nu = 0.750 \pm 0.003$. However, the former value is larger than the theoretically predicted value $\nu = 0.63$ of the Ising model. We will discuss possible reasons for this discrepancy below. The crossover between these two regimes is again analogous to previous results obtained when approaching the critical point of polymer solutions by lowering the temperature.[28,29]

Above, we determined the scaling exponent μ for the interfacial tension; see Figure 8B. Scaling considerations following eqs 6 and 7 suggest that μ is related to the scaling exponent ν via

$$\mu = 1 + \nu \tag{8a}$$

from mean field theory and

$$\mu = 2\nu \tag{8b}$$

from the theory of critical phenomena. When the theoretical values for ν, i.e., $\nu = 0.63$ and $1/2$ in the Ising and mean field regimes, respectively, are inserted into these expressions, one obtains the scaling exponent $\mu = 1.26$ in the Ising regime and $\mu = 3/2$ in the mean field regime. As shown in Figure 8B, the latter value of μ agrees very well with the experimental value of 1.50 ± 0.01, but the former value disagrees with the experimental value of 1.67 ± 0.10. In contrast, the scaling exponent β in Figure 9 showed a crossover from a value close to the Ising limit of $\beta = 0.326$ to mean field behavior with $\beta = 1/2$. Therefore, in the Ising limit region, there seems to be a discrepancy for the observed scaling exponents $\mu = 1.67 \pm 0.10$ and $\nu = 0.835 \pm 0.051$ with the corresponding theoretical values of $\mu = 1.26$ and $\nu = 0.63$. This deviation from the expected asymptotic behavior could reflect gravity or impurity effects as discussed in refs 40 and 41. The observed discrepancy could also arise from the polydispersity of the polymers (the polydispersities of dextran and PEG are 1.83 and 1.11, respectively), i.e., the quasi-ternary composition of the system. It was shown that, during phase separation, the polymer components with lower molar mass fractionate into the polymer-poor phase rather than the polymer-rich phase.[42] The correlation length is thus expected to decrease (see, e.g., ref 28) because of adsorption of low molar mass components at the two-phase interface. As one approaches the critical point by decreasing the polymer concentration, the fractionation effect becomes weaker and the correlation length increases more rapidly, resulting in a steeper decrease of the interfacial tension. Thus, this fractionation effect provides a possible explanation for the higher values $\mu = 1.67 \pm 0.10$ and $\nu = 0.835 \pm 0.051$ compared to the theoretical values in the Ising limit. However, the fractionation does not affect the polymer concentration in the coexisting phases since the polymer density does not depend on the molar mass. Thus, the scaling exponent β for the order parameter is observed to move closer toward its Ising value $\beta = 0.326$ as one approaches the critical point; see Figure 9.

From Figures 8−10, we conclude that the crossover region observed for the interfacial tension, the order parameters, and the correlation length is located in the concentration range $0.1 \leq \varepsilon \leq 0.2$. To elucidate the molecular mechanism behind the crossover, we compared the radii of gyration R_g of the two polymers and the correlation lengths ξ_d^D and ξ_p^P of the concentration fluctuations of dextran in the dextran-rich phase and PEG in the PEG-rich phase, with the correlation length of the compositional fluctuations ξ; see Figure 10. Because the demixed polymer phases are both in the semidilute regime, for the polymer in the phase rich in the same species (dextran in the dextran-rich phase and PEG in the PEG-rich phase), the correlation length can be calculated according to[43]

$$\xi_d^D = \sqrt{6}\, R_{g,d} (c_d^D/c_d^*)^{-\nu_F/(3\nu_F-1)} \tag{9a}$$

$$\xi_p^P = \sqrt{6}\, R_{g,p} (c_p^P/c_p^*)^{-\nu_F/(3\nu_F-1)} \tag{9b}$$

where $c^* = 3M_w/4\pi N_A R_g^3$ is the overlapping concentration and $\nu_F = 0.588$.

It can be seen that the crossover between the two regimes is located where the correlation length is on the order of the length scale of the coexisting phases. Far from the critical point the interfacial thickness is about the size of the polymer correlation length, while closer to the critical point this length scale increases, which causes a decrease in the interfacial

dx.doi.org/10.1021/la204757z | Langmuir 2012, 28, 3831−3839

tension. Previous neutron scattering and light scattering experiments have shown that the crossover is at a correlation length equal to the normalized radius of gyration $R_g/3^{1/2}$.[28,29] Far away from the critical point, the correlation length is smaller than the normalized radius of gyration of the polymer. Thus, the compositional fluctuations are screened, and mean field behavior is expected. When approaching the critical point, the correlation length ξ diverges and becomes larger than the normalized radius of gyration of the polymer and Ising behavior is expected. It would therefore be interesting to measure the correlation length of our system and compare it with the estimates presented in Figure 10.

To further compare our results with the theory of crossover from critical to tricritical behavior of polymer solutions,[44] we plot in Figure 11 the coexistence curves of the polymer solutions. The reduced polymer concentrations of dextran in the dextran- and PEG-rich phases, $\varepsilon_d^{D,P} = |c_d^{D,P}/c_{cr,d} - 1|$, and of PEG in the dextran- and PEG-rich phases, $\varepsilon_p^{D,P} = |c_p^{D,P}/c_{cr,p} - 1|$, as functions of the reduced concentration ε are shown separately. Theoretically, for dextran the dextran-rich phase is the polymer-rich phase, while the PEG-rich phase is the solvent-rich phase. For PEG, the dextran-rich phase is theoretically the solvent-rich phase, while the PEG-rich phase is the polymer-rich phase. It can be seen that the data in the low concentration range approximate the Ising limit with the scaling exponent of the order parameter $\beta = 0.326$, while the highest polymer concentration explored approaches the tricritical limit with $\beta = 1$ (where the correlation length ξ is smaller than the radius of gyration of the polymer; see Figure 10). Overall, the data are very similar to phase-coexistence curves of polymer solutions at temperatures below the critical one, indicating that the crossover theory is also applicable to the aqueous two-phase polymer systems studied here.

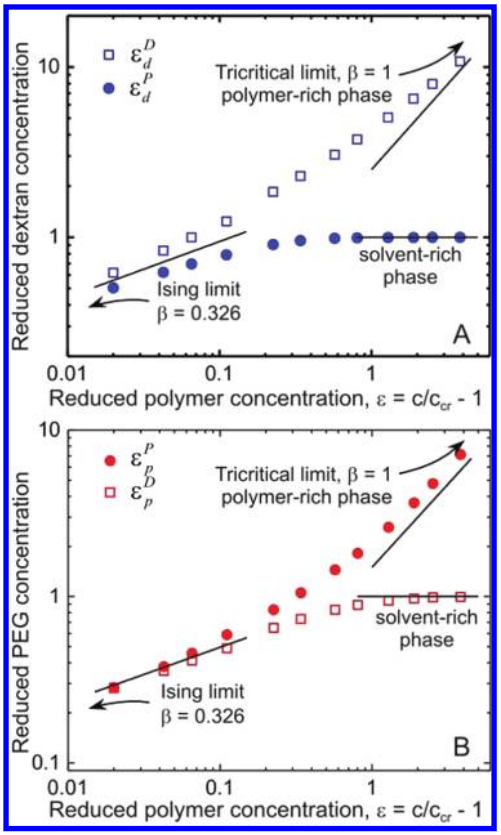

Figure 11. Logarithmic scaling plots of phase-coexistence curves for (A) dextran and (B) PEG. The solid lines are guides to the eye with scaling exponents of 0.326 for the Ising model limit and 1 for the tricritical limit and a constant of 1 for the solvent-rich phase.

CONCLUSIONS

Phase separation of aqueous solutions of dextran and PEG were studied over a broad range of concentrations above the critical point. The interfacial tensions of the coexisting phases were measured by a spinning drop tensiometer. It was found that the scaling exponent of the interfacial tension with the distance to the critical concentration gives a value of 1.67 ± 0.10 close to the critical point and another value of 1.50 ± 0.01 far away from it. The latter value agrees with the mean field value 3/2 whereas the value 1.67 disagrees with the Ising model value 1.26, see Figure 8, a discrepancy that might arise from polymer fractionation during phase separation. The composition and density differences, on the other hand, do exhibit the expected crossover from mean field to Ising model behavior as the critical point is approached, see Figure 9.

AUTHOR INFORMATION

Corresponding Author

*E-mail: yonggang.liu@mpikg.mpg.de (Y.L.); rumiana.dimova@mpikg.mpg.de (R.D.). Phone: +49 331 5679615. Fax: +49 331 5679612.

Present Address

†State Key Laboratory of Polymer Physics and Chemistry, Changchun Institute of Applied Chemistry, Chinese Academy of Sciences, 130022 Changchun, People's Republic of China.

Notes

The authors declare no competing financial interest.

ACKNOWLEDGMENTS

Y.L. thanks Yanhong Li for her help at the early stage of the experiment.

REFERENCES

(1) Albertsson, P. Å. *Partition of Cell Particles and Macromolecules: Separation and Purification of Biomolecules, Cell Organelles, Membranes, and Cells in Aqueous Polymer Two-Phase Systems and Their Use in Biochemical Analysis and Biotechnology*, 3rd ed.; Wiley: New York, 1986; 346 pp.

(2) Ryden, J.; Albertsson, P. Å. *J. Colloid Interface Sci.* **1971**, *37* (1), 219−222.

(3) Forciniti, D.; Hall, C. K.; Kula, M. R. *J. Biotechnol.* **1990**, *16* (3−4), 279−296.

(4) Forciniti, D.; Hall, C. K.; Kula, M. R. *Fluid Phase Equilib.* **1991**, *61* (3), 243−262.

(5) Abbott, N. L.; Blankschtein, D.; Hatton, T. A. *Macromolecules* **1991**, *24* (15), 4334−4348.

(6) Cesi, V.; Katzbauer, B.; Narodoslawsky, M.; Moser, A. *Int. J. Thermophys.* **1996**, *17* (1), 127−135.

(7) Zhou, H. X.; Rivas, G. N.; Minton, A. P. *Annu. Rev. Biophys.* **2008**, *37*, 375−397.

(8) Helfrich, M. R.; Mangeney-Slavin, L. K.; Long, M. S.; Djoko, Y.; Keating, C. D. *J. Am. Chem. Soc.* **2002**, *124* (45), 13374−13375.

(9) Dimova, R.; Aranda, S.; Bezlyepkina, N.; Nikolov, V.; Riske, K. A.; Lipowsky, R. *J. Phys.: Condens. Matter* **2006**, *18* (28), S1151−S1176.

(10) Li, Y.; Lipowsky, R.; Dimova, R. *J. Am. Chem. Soc.* **2008**, *130* (37), 12252−12253.

(11) Long, M. S.; Jones, C. D.; Helfrich, M. R.; Mangeney-Slavin, L. K.; Keating, C. D. *Proc. Natl. Acad. Sci. U.S.A.* **2005**, *102* (17), 5920−5925.
(12) Long, M. S.; Cans, A. S.; Keating, C. D. *J. Am. Chem. Soc.* **2008**, *130* (2), 756−762.
(13) Kusumaatmaja, H.; Li, Y.; Dimova, R.; Lipowsky, R. *Phys. Rev. Lett.* **2009**, *103* (23), 238103.
(14) Andes-Koback, M.; Keating, C. D. *J. Am. Chem. Soc.* **2011**, *133* (24), 9545−9555.
(15) Li, Y.; Lipowsky, R.; Dimova, R. *Proc. Natl. Acad. Sci. U.S.A.* **2011**, *108* (12), 4731−4736.
(16) Ioan, C. E.; Aberle, T.; Burchard, W. *Macromolecules* **2000**, *33* (15), 5730−5739.
(17) Devanand, K.; Selser, J. C. *Macromolecules* **1991**, *24* (22), 5943−5947.
(18) Koningsveld, R.; Staverma, A. J. *J. Polym. Sci., Polym. Phys. Ed.* **1968**, *6* (2), 325−347.
(19) Vonnegut, B. *Rev. Sci. Instrum.* **1942**, *13* (1), 6−9.
(20) Princen, H. M.; Zia, I. Y. Z.; Mason, S. G. *J. Colloid Interface Sci.* **1967**, *23* (1), 99−107.
(21) Kang, C. H.; Sandler, S. I. *Macromolecules* **1988**, *21* (10), 3088−3095.
(22) Kaul, A. *Aqueous Two-Phase Systems: Methods and Protocols*; Humana Press: Totowa, NJ, 2000; Vol. *11*, pp 11−21.
(23) King, R. S.; Blanch, H. W.; Prausnitz, J. M. *AIChE J.* **1988**, *34* (10), 1585−1594.
(24) Diamond, A. D.; Hsu, J. T. *Biotechnol. Tech.* **1989**, *3* (2), 119−124.
(25) Michielsen, S. In *Polymer Handbook*; Brandrup, J., Immergut, E. H., Grulke, E. A., Abe, A., Bloch, D. R., Eds.; John Wiley & Sons: New York, 2003.
(26) Sanchez, I. C. *J. Phys. Chem.* **1989**, *93* (19), 6983−6991.
(27) Widom, B. *Physica A* **1993**, *194* (1−4), 532−541.
(28) Melnichenko, Y. B.; Anisimov, M. A.; Povodyrev, A. A.; Wignall, G. D.; Sengers, J. V.; van Hook, W. A. *Phys. Rev. Lett.* **1997**, *79* (26), 5266−5269.
(29) Anisimov, M. A.; Kostko, A. F.; Sengers, J. V. *Phys. Rev. E* **2002**, *65* (5), 051805.
(30) Dobashi, T.; Nakata, M.; Kaneko, M. *J. Chem. Phys.* **1980**, *72* (12), 6692−6697.
(31) Shinozaki, K.; Vantan, T.; Saito, Y.; Nose, T. *Polymer* **1982**, *23* (5), 728−734.
(32) Heinrich, M.; Wolf, B. A. *Polymer* **1992**, *33* (9), 1926−1931.
(33) Ginzburg, V. L. *Sov. Phys. Solid State* **1961**, *2* (9), 1824−1834.
(34) Hong, K. M.; Noolandi, J. *Macromolecules* **1981**, *14* (3), 736−742.
(35) Broseta, D.; Leibler, L.; Kaddour, L. O.; Strazielle, C. *J. Chem. Phys.* **1987**, *87* (12), 7248−7256.
(36) Scholten, E.; Tuinier, R.; Tromp, R. H.; Lekkerkerker, H. N. W. *Langmuir* **2002**, *18* (6), 2234−2238.
(37) Marszalek, P. E.; Oberhauser, A. F.; Pang, Y. P.; Fernandez, J. M. *Nature* **1998**, *396* (6712), 661−664.
(38) Kienberger, F.; Pastushenko, V. P.; Kada, G.; Gruber, H. J.; Riener, C.; Schindler, H.; Hinterdorfer, P. *Single Mol.* **2000**, *1* (2), 123−128.
(39) Rowlinson, J. S.; Widom, B. *Molecular Theory of Capillarity*; Clarendon Press: Oxford, U.K., 1989.
(40) Fameli, N.; Balzarini, D. A. *Phys. Rev. B* **2007**, *75* (6), 064203.
(41) Wang, J.; Cerdeirina, C. A.; Anisimov, M. A.; Sengers, J. V. *Phys. Rev. E* **2008**, *77*, 3.
(42) Edelman, M. W.; van der Linden, E.; Tromp, R. H. *Macromolecules* **2003**, *36* (20), 7783−7790.
(43) de Gennes, P.-G. *Scaling Concepts in Polymer Physics*; Cornell University Press: Ithaca, NY, 1979; 324 pp.
(44) Anisimov, M. A.; Agayan, V. A.; Gorodetskii, E. E. *JETP Lett.* **2000**, *72* (11), 578−582.